Antiperovskites

International Edition: DOI: 10.1002/anie.201603920
German Edition: DOI: 10.1002/ange.201603920

Metal Vacancy Ordering in an Antiperovskite Resulting in Two Modifications of Fe_2SeO

Martin Valldor, Taylor Wright, Andrew Fitch, and Yurii Prots*

Abstract: *Small, red Fe_2SeO single crystals in two modifications were obtained from a CsCl flux. The metastable α-phase is pseudo-tetragonal (Cmce, $a = 16.4492(8)$ Å, $b = 11.1392(4)$ Å, $c = 11.1392(4)$ Å), whereas the β-phase is trigonal ($P3_1$, $a = 9.8349(4)$ Å, $c = 6.9591(4)$ Å)) and thermodynamically stable within a narrow temperature range. Both crystal structures were solved from twinned specimens. The enantiomers of the β-phase appear as racemic mixtures. Selenium and oxygen form two individual interpenetrating primitive cubic lattices, giving a bcc packing. A quasi-octahedrally coordinated iron atom is found close to the center of each surface of the selenium sublattice. The difference between the α- and β-phases is the distribution of iron at 2/3 of the surfaces. α- and β-Fe_2SeO are comparable with metal-vacancy-ordered antiperovskites. Each Fe/O lattice can also be described in terms of vertex-sharing OFe_4 tetrahedra, with a crystal structure similar to that of an antisilicate. Iron is divalent and has a high-spin d^6 ($S = 2$) configuration. The β-phase exhibits magnetoelectric coupling.*

Combinations of chalcogens with iron are receiving increasing attention owing to the superconductivity of non-stoichiometric $Fe_{1+x}Se$ with α-PbO structure, which consists of a cubic close packed (ccp) anionic lattice.[1] The iron-containing mineral pentlandite also has a ccp anionic lattice and deviates from 1:1 stoichiometry, TM_9S_8 (TM = Fe, Ni, Co).[2] On the contrary, the stoichiometric materials FeS,[2] FeSe,[2] and FeTe[3] exhibit a NiAs-type structure with hexagonally close packed (hcp) anions and can be described as semiconductors (S) or metals (Se, Te). Wüstite, $Fe_{1-x}O$, is non-stoichiometric,[4] has a ccp anionic lattice, behaves as a semiconductor, and is metastable at room temperature.[4] However, the combination of two chalcogens with Fe in a ternary compound has, up to now, been limited to solid solutions such as $FeTe_{0.5}Se_{0.5}$,[5] which is related to the superconducting α-PbO phase. The bimorphic title compound, Fe_2SeO, is surprisingly different and results from combining Fe with two chalcogenides with a larger ionic size difference, Se^{2-} and O^{2-}, causing a structural ordering of the anions. A well-known, but today less practiced, synthesis method was used to obtain single crystals of up to 70 μm (Figure 1) of two different Fe_2SeO modifications: Powders of Fe metal, Fe_2O_3, and Se were reacted in a CsCl melt under inert conditions inside a closed, evacuated silica vessel. After rinsing the sample with water, the bulk sample was still impure, with several crystalline phases being detected by powder X-ray diffraction. The two Fe_2SeO modifications could be separated according to their outer shape and place of formation; one can be described as capped square pyramids (α in Figure 1), and is found on the inner silica tube wall above the reaction mixture. The other phase, consisting of square prisms, was dominating in the solidified salt melt (β in Figure 1). Single crystals of a third compound, $[Cs_6Cl][Fe_{24}Se_{26}]$, were also found in the sample, but this is discussed elsewhere.[6] Extensive optimization of the solid-state reaction afforded samples where different modifications dominated (see the Supporting Information, Section S1), but high purities were not achieved. By investigating samples that were quenched at different reaction temperatures, the α-phase proved to be metastable whereas the β-phase is stable within a narrow temperature range (Section S2).

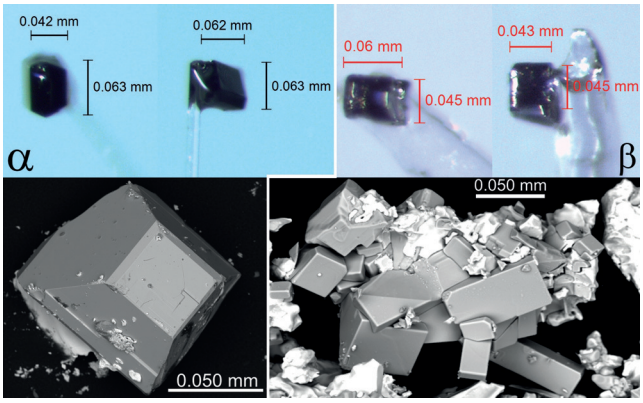

Figure 1. Top: The crystallites used for the X-ray experiments. Bottom: Back-scattering scanning electron microscope images of the as-grown crystals with the CsCl flux matrix.

The Fe/Se ratio was determined to be approximately 2.05(4):0.95(2) by basic elemental analysis and energy-dispersive X-ray analysis, which corresponds to the average from both modifications. The tilting of the surfaces (Figure 1) and the charging of the crystals prevented an accurate oxygen elemental analysis. However, all three elements (Fe, Se, O) were detected, without inclusion of Cs or Cl.

[*] Dr. M. Valldor, T. Wright, Dr. Yu. Prots
Max Planck Institute for Chemical Physics of Solids
01187 Dresden (Germany)
E-mail: martin.valldor@cpfs.mpg.de
Prof. Dr. A. Fitch
ESRF, The European Synchrotron
71 Avenue des Martyrs, 38000 Grenoble (France)
Supporting information and the ORCID identification numbers for the authors of this article can be found under http://dx.doi.org/10.1002/anie.201603920.

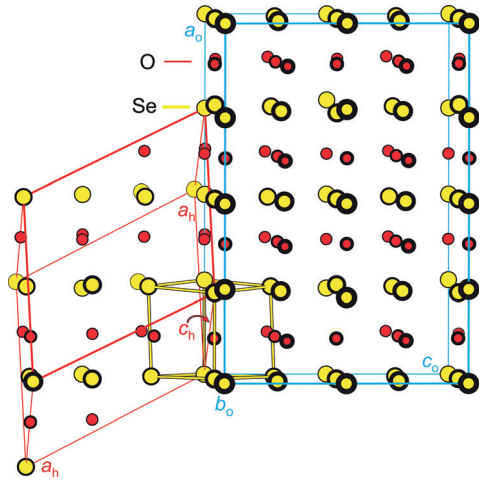

Figure 2. The anion bcc lattices in the α and β-modifications. The unit cells of both modifications were set relative to the common anionic lattice and to an idealized perovskite unit cell, represented by an Se_8 cube.

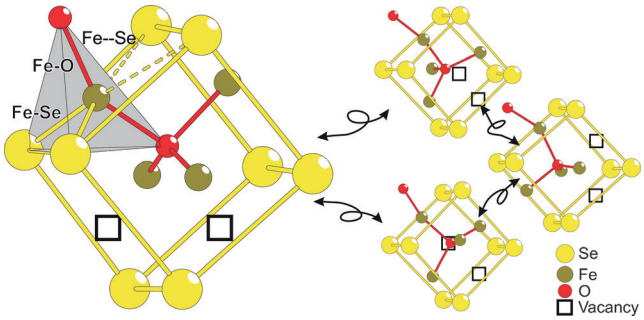

Figure 3. The four *cis* configurations of OFe_4 in an Se_8 cube with one fixed Fe site. The quasi-tetrahedral coordination of Fe is also displayed, with reasonable bonds shown as full lines and with dashed lines for distances that are considered too long for bonding.

The anionic bcc lattices in α- and β-Fe_2SeO can be described as interpenetrating primitive cubic lattices of Se and O (Figure 2). The mean distances of $d(Se–O) = 3.463(6)$ Å in the α-phase and 3.488(2) Å in the β-phase are close to the expected value, that is, the sum of the ionic radii ($r(Se^{2-}) = 1.98$ Å, $r(O^{2-}) = 1.42$ Å).[7] Furthermore, the d(Se–Se) distances range from 3.72 to 4.29 Å in the α-phase and from 3.92 to 4.09 Å in the β-phase, in agreement with a close-packed structure. The shortest d(Se–Se) distance, which was found in the α-modification, is still significantly larger than the corresponding bond length in a perselenide ion, which is 2.61 Å in $FeSe_2$, for example.[8] Hence, in Fe_2SeO, all Se ions are present as Se^{2-}. The d(O–O) distance, which is similar to d(Se–Se), is too long for true close packing, in line with the reason why bcc is different from ccp and hcp. Trying to describe the β-Fe_2SeO structure with another packing model, for example, with layers of $[Fe_6Se_3\square_3]^{6+}$ having 1/4 vacancies (□), cubic stacking, and 1/8 of the tetrahedral voids occupied by O (almost SnI_4-type)[9] results in a complex situation, and the α-phase is additionally complicated by its layered structure and different vacancy distribution. Hence, if simplicity is of essence, the bcc description of Se and O is preferred. Homogenous anion bcc lattices have been reported for α-AgI[10] and α-CuBr,[11] but the cations involved were found on split positions as a result of structural disorder. Even more similar to the title compound is the antiperovskite Ag_3SI, where the same anion ordering as in Fe_2SeO evolves into a bcc lattice.[12]

Within the bcc anionic lattice, Fe is found close to the surfaces of the Se squares with possible coordination to four Se and two O ions (Figure 3). As the high-symmetry site seems to be too large for the Fe^{2+} ion, the metal ion is slightly shifted and assumes a lower coordination number. Alternatively, the coordination can be described in terms of an O ion that is situated close to the Se cube center, but slightly shifted towards the four Fe ions, which leads to distorted OFe_4 tetrahedral coordination (Figure 3). In accordance with the composition, only four of six surfaces of the Se cube are occupied by Fe, and the other two sites are vacant (Figure 3). The two vacancies are always found on neighboring surfaces, as if the system tries to avoid an OFe_4 square planar coordination in both modifications of Fe_2SeO. The Fe vacancies are ordered in different ways in the α- and β-modifications. Hence, the ordering of the Fe site vacancies (□) is decisive for the crystal symmetry, rendering it orthorhombic (or pseudo-tetragonal) in the α-phase and chiral, polar, non-centrosymmetric, and trigonal in the β-modification (Figure 4). The unit cell relations between

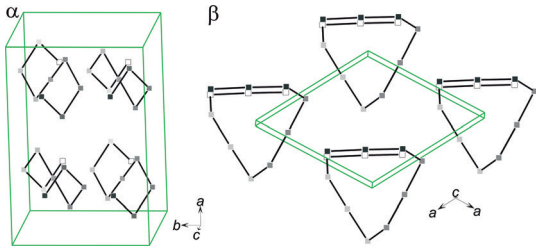

Figure 4. The vacancy (□) distribution relative to the unit cells of both Fe_2SeO modifications. Lines connect the nearest vacancies, and the boxes are darker if they are closer to the reader.

the structures reported here and a perovskite subcell ($a_p \approx Se_8$ cube), shown in Figure 2, are as follows: [400, 220, 0$\bar{2}$2] for α-Fe_2SeO ($a = 4 \times a_p$, $b = 2\sqrt{2} \times a_p$, and $c = 2\sqrt{2} \times a_p$) and [2$\bar{1}$1, $\bar{1}$21, 111] for β-Fe_2SeO ($a = \sqrt{3} \times \sqrt{2} \times a_p$ and $c = \sqrt{3} \times a_p$).

Although only impure powders of the title compounds have been obtained thus far, a sample predominantly containing the α-phase (ca. 85% phase-pure) was investigated with synchrotron X-rays to confirm the unit cell, which could be either pseudo-tetragonal or orthorhombic (Section S1). As no splitting was observed for the relevant Bragg intensities, for example, [0 8 0], the pseudo-tetragonal ($a \neq b = c$) description is a representative model and stems from the layered nature of the α-phase: Each layer has a quasi-fourfold rotational symmetry. By superimposing two neighboring layers (Section S5), it becomes obvious that a relative in-plane shift breaks the global fourfold symmetry and results in the C-centered orthorhombic symmetry.

The ordering of the metal vacancies, which is responsible for the unit cell size and symmetry, has been well investigated for the solid-state compounds $Ti_{1-x}O$, with Ti_9O_{10} and Ti_4O_5,[13] for example, being well defined vacancy-related superstructures of the NaCl type. The hypothetical title compound without vacancies, "Fe_3SeO", would be an antiperovskite, similar to $Fe_3(TM)N$ (TM = Ni, Pt)[14] or Fe_3MC (M = Zn, Sn),[15] but in the title compound, the vacancies are necessary for charge balance. A low-temperature study of the ionic conductor Ag_3SI revealed an average crystal structure that is similar to a strongly distorted antiperovskite with a polar, non-centrosymmetric *R*3 space-group description.[16] Hence, the title compounds can be described as being structurally related to the low-temperature phase γ-Ag_3SI, but with vacancies on one third of the transition-metal sites. The metal vacancy ordering in Fe_2SeO allows for the development of ground-state degeneracy: An OFe_4 tetrahedron with one corner fixed in the Se_8 cube can still adopt eight different orientations, of which the four *cis* configurations are displayed in Figure 3. This degeneracy is the reason for finding at least the two different modifications presented here.

The distances between Fe and its nearest neighbors in both modifications of Fe_2SeO are reasonable for ionic bonding (Figure 3): d(Fe–O) = 1.94–2.01 Å, d(Fe–Se) = 2.50–2.77 Å, and d(Fe–Se) = 2.83–3.33 Å. These are comparable with the $d(Fe^{2+}–O^{2-})$ bond lengths of 1.95–2.17 Å that are observed in the well-defined ionic structure of ilmenite $FeTiO_3$,[17] and the d(Fe–Se) bond length in FeSe is typically 2.56 Å.[2] The fact that the Fe–Se distances in Fe_2SeO have an ill-defined limit between short (——) and long (– – –) bonds (Figure 3) leaves Fe with a coordination number of four or five. A more satisfying bonding description is realized in the anti-structure of vertex-connected OFe_4 tetrahedra (Figures 3 and 5). Thus α-Fe_2SeO can be written as $^2_\infty[OFe_{4/2}]^{2+}[Se]^{2-}$ and β-Fe_2SeO as $^3_\infty[OFe_{4/2}]^{2+}[Se]^{2-}$, demonstrating that the most obvious difference between the two modifications is the dimensionality of the Fe/O tetrahedral network.

When examining the Fe/O network in both modifications of Fe_2SeO more closely, it is evident that the α-structure contains four- and eight-membered rings of OFe_4 tetrahedra (Figure 5), whereas the β-structure consists of four- and six-membered rings. Six-membered rings of tetrahedra are often found in silicates, for example, in the low-pressure modification of SiO_2, α-quartz (Section S6).[18] A "stuffed" version of a quartz-like structure was realized in $BaZnO_2$,[19] which was chemically extended with Co and Mn.[20] In this structure, Ba^{2+} was filled into the large void in the six-membered ring and assumed an eightfold O coordination (Section S6). Although the ring of OFe_4 tetrahedra in β-Fe_2SeO is folded differently, Se^{2-} enters the void in a six-membered ring and coordinates to eight Fe irons (Section S6). Hence, it is fair to describe at least β-Fe_2SeO as a filled antisilicate as an alternative to metal-vacancy-ordered antiperovskite.

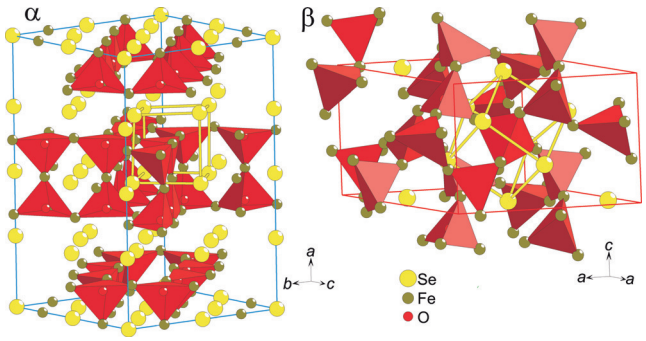

Figure 5. Perspective views of the complete crystal structures of α-Fe_2SeO and β-Fe_2SeO, with the OFe_4 tetrahedra highlighted and the unit cells added. One Se_8 cube is marked in each modification to emphasize the perovskite sublattice.

In crystal structures with large voids with negatively charged coordination spheres, hydrogen inclusion might be suspected, which is not resolved by X-ray diffraction. However, any hydrogen ions in the vacancies of the title compounds would reduce the oxidation of Fe to less than +2, and the +1 state is highly unlikely considering the insulating nature of the title compound. Hence, the Fe vacancies are assumed to be completely unoccupied.

The title compound carries features from strongly correlated systems with highly ionic character, as judged by the interatomic bond lengths and coordination numbers. Yet, the crystal structure rather fits to anti-type structure descriptions, where far less electronic correlations, or even metallic behavior, are commonly observed. This unique electronic cross-over character might be related to the rare mixture of the involved anions (O^{2-} and Se^{2-}), forming an intimate 3D-ordered lattice, and the metal vacancies, which are a result of charge balance.

The close structural relation of $Fe_2\square SeO$ and Ag_3SI and their structural diversities imply that the title compounds might be Fe^{2+} ionic conductors. The fact that vacancies exist on possible Fe sites only underlines this possibility, as the best O^{2-} ion conductors, for example, δ-Bi_2O_3[21,22] and yttria-stabilized zirconia (YSZ),[23,24] have oxygen-deficient fluorite structures. Furthermore, the tetrahedral slabs in the oxygen-ion-conducting brownmillerites,[25,26] for example, Ca_2FeAlO_5, even have a close anti-type structural relation with the title compounds. A preliminary thermodynamic investigation of a powder sample (Section S2) also supports the high mobility of Fe: The α- to β-phase transition seems to be continuous because no entropy release was observed below the reversible decomposition of the title compound. If Fe_2SeO proves to be an iron ion conductor, it is probably the first example of ionic conductivity for magnetic ions.

From our crystal structure twin analysis of the β-modification specimen, shown in Figure 1, the chirality of the major domain (89 %) is right-handed ($P3_1$, No. 144), and the minor domain (11 %) is left-handed ($P3_2$, No. 145). Chiral crystal structures are still relatively rare, especially for ionic inorganic compounds obtained through synthesis in a laboratory. Other investigated crystals show different $P3_1/P3_2$ ratios or even prevalent left-handed chirality. Hence, it is important to note that there seems to be no chirality preference in β-Fe_2SeO. This can be expected as the crystal growth was performed in the absence of possible influences from strong magnetic or electric fields.

As judged from the red color of the powder, the title compounds should be insulating, suggesting the presence of

Fe^{2+} (d^6). In combination with the small crystal field from the quasi-tetrahedral coordination, Fe should have a high-spin ($S=2$) configuration. Preliminary magnetic data indicate that the Fe_2SeO modifications (Figures 6, S7, and S8) behave differently. In the paramagnetic temperature range, the β-modification exhibits a μ_{eff}(Fe) value of 4.45 μ_B, which is close to the expected value of 4.9 μ_B for $S=2$ (S8). α-Fe_2SeO displays a sudden drop in the χ value close to $T_N=125$ K, which might be the Verwey transition of the magnetite impurity[27] or, perhaps, an intrinsic antiferromagnetic-like spin ordering. β-Fe_2SeO, with its chiral, polar, non-centrosymmetric space group, exhibits a possible spin ordering at about $T_C=110$ K and a sharp spin reorientation effect at $T_N=78$ K. This mimics the behavior of α-Fe_2O_3, where a canted antiferromagnetic state sets in at 953 K, and the Morin transition is observed at 260 K.[28] This is possibly due to magnetoelectric coupling in β-Fe_2SeO, in line with discussions for α-Fe_2O_3. Larger single crystals and pure powder samples are needed to complete the physical investigations.

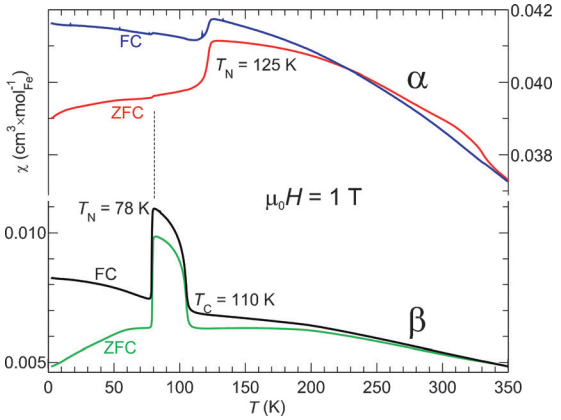

Figure 6. Temperature-dependent magnetic susceptibility (χ) of the purest powder samples of α- and β-Fe_2SeO. FC and ZFC designate field-cooling and zero-field-cooling data, respectively. The temperatures of some curve anomalies are indicated. The dashed line indicates a common magnetic feature.

Experimental Section

Small single crystals were grown in a CsCl flux inside an evacuated silica ampoule. A mixture with powders of Fe, Se, SeO_2, and CsCl in a molar ratio of 4:1:1:3 was heated to 750 °C over 6 hours. Subsequently this temperature was held for 96 h, and then lowered to 500 °C during 96 h before the furnace was switched off. The well-shaped crystals were separated from the CsCl by rinsing with deionized water. The two modifications could be separated according to their outer shape.

Single-crystal data were obtained with a Bruker D8 Quest diffractometer, working with a CMOS detector (Photon), and a Mo Kα X-ray source ($\lambda=0.71073$ Å). Details on the crystal-structure refinements are given in the Supporting Information (Sections S3 and S4). Magnetic data were obtained with an MPMS XL from Quantum Design. A scanning electron microscope (SEM XL30) with an attached energy-dispersive X-ray spectrometer (EDX) from Philips working at 25 kV was used for elemental analysis.

Acknowledgements

We are very grateful to Rüdiger Kniep for initial reviewing and for his many suggestions to improve the manuscript. We also thank Liu Hao Tjeng and Yuri Grin for their invaluable comments. Petra Scheppan and Ulrich Burkhardt are acknowledged for electron microscopy studies (EDX), and we thank Marcus Schmidt and Susann Scharsach for obtaining differential scanning calorimetry (DSC) data.

Keywords: antiperovskites · chirality · crystal growth · magnetic properties · X-ray diffraction

How to cite: *Angew. Chem. Int. Ed.* **2016**, *55*, 9380–9383
Angew. Chem. **2016**, *128*, 9526–9529

[1] F.-C. Hsu, J.-Y. Luo, K.-W. Yeh, T.-K. Chen, T.-W. Huang, P. M. Wu, Y.-C. Lee, Y.-L. Huang, Y.-Y. Chu, D.-C. Yan, M.-K. Wu, *Proc. Natl. Acad. Sci. USA* **2008**, *105*, 14262–14264.
[2] N. Alsén, *Geol. Foeren. Stockholm Foerh.* **1925**, *47*, 19–73.
[3] I. Oftedal, *Z. Phys. Chem.* **1927**, *132*, 208–216.
[4] R. W. G. Wyckoff, E. D. Crittenden, *Z. Kristallogr. Kristallgeom. Kristallphys. Krista* **1926**, *63*, 144–147.
[5] K. Horigane, H. Hiraka, K. Ohoyama, *J. Phys. Soc. Jpn.* **2009**, *78*, 074718.
[6] M. Valldor, B. Böhme, Yu. Prots, H. Borrmann, P. Adler, W. Schnelle, Y. Watier, C.-Y. Kuo, T.-W. Pi, Z. Hu, C. Felser, L. H. Tjeng, *Chem. Eur. J.* **2016**, *22*, 4626–4631.
[7] R. D. Shannon, *Acta Crystallogr. Sect. A* **1976**, *32*, 751–767.
[8] S. Tengner, *Z. Anorg. Allg. Chem.* **1938**, *239*, 126–132.
[9] H. Ott, *Z. Kristallogr. Kristallgeom. Kristallphys. Krista* **1926**, *63*, 222–230.
[10] S. Hoshino, *J. Phys. Soc. Jpn.* **1957**, *12*, 315–326.
[11] J. Krug, L. Sieg, *Z. Naturforsch. A* **1952**, *7*, 369–371.
[12] B. Reuter, K. Hardel, *Naturwissenschaften* **1961**, *48*, 161–161.
[13] E. Hilti, *Naturwissenschaften* **1968**, *55*, 130–131.
[14] G. W. Wiener, J. A. Berger, *J. Metals* **1955**, *7*, 360–368.
[15] H. H. Stadelmaier, L. J. Huetter, *Acta Metal.* **1959**, *7*, 415–419.
[16] X. H. Honda, K. Basar, S. Siagian, T. Sakuma, H. Takahashi, Tubuqinbaer, H. Kawaji, T. Atake, *J. Phys. Soc. Jpn.* **2007**, *76*, 114603.
[17] T. F. W. Barth, E. Posnjak, *Z. Kristallogr. Kristallgeom. Kristallphys. Krista* **1934**, *88*, 265–270.
[18] W. H. Bragg, *Proc. R. Soc. London Ser. A* **1914**, *89*, 575–580.
[19] H. G. von Schnering, R. Hoppe, J. Zemann, *Z. Anorg. Allg. Chem.* **1960**, *305*, 241–248.
[20] U. Spitsbergen, *Acta Crystallogr.* **1960**, *13*, 197–198.
[21] G. Gattow, H. Schröder, *Z. Anorg. Allg. Chem.* **1962**, *318*, 176–189.
[22] M. Yashima, D. Ishimura, *Chem. Phys. Lett.* **2003**, *378*, 395–399.
[23] M. Morinaga, J. B. Cohen, *Acta Crystallogr. Sect. A* **1979**, *35*, 789–795.
[24] D.-J. Kim, *J. Am. Ceram. Soc.* **1989**, *72*, 1415–1421.
[25] A. A. Colville, S. Geller, *Acta Crystallogr. Sect. B* **1971**, *27*, 2311–2315.
[26] A. L. Shaula, Y. V. Pivak, J. C. Waerenborgh, P. Gacyzñski, A. A. Yaremchenko, V. V. Kharton, *Solid State Ionics* **2006**, *177*, 2923–2930.
[27] E. J. W. Verwey, *Nature* **1939**, *144*, 327–328.
[28] Ö. Özdemir, D. J. Dunlop, *Geophys. Res.* **2006**, *111*, B12S03.

Received: April 22, 2016
Published online: June 16, 2016

